

Beam Pattern Characterization of the 6-M TIGO Telescope

*Felipe Pedreros*¹, *Hugo Pacheco*², *Hayo Hase*³

¹⁾ *Transportable Integrated Geodetic Observatory TIGO, Universidad de Concepción.*

²⁾ *Center for Optics and Photonics and Departamento de Ingeniería Eléctrica, Universidad de Concepción.*

³⁾ *Bundesamt für Kartographie und Geodäsie.*

Contact author: Felipe Pedreros, e-mail: felipe.pedreros@tigo.cl

Abstract

We present an investigation to characterize the beam pattern of the 6-m telescope at TIGO. The near-field and the far-field beam patterns were measured in X-band (8.4 GHz), in order to experimentally verify the shape of the beam and to detect the existence of sidelobes.

1. Introduction

The beam pattern or radiation pattern of an antenna is one of its most important characteristics, representing the directional dependence of the radiated or received power. The beam pattern of an antenna can be separated in two, namely the near-field pattern and the far-field pattern. While the near-field pattern is referred to the radiation pattern within the Fresnel zone where it is also dependent on the distance to the antenna, the far-field pattern corresponds to that beyond these points, and it is completely independent of the distance to the antenna [1].

TIGO has a 6-m offset radio telescope with a dual band receiver used for VLBI experiments [2]. The far-field beam pattern of the telescope has been computed by the feed manufacturer ERA Technology by means of the experimental measurements of the feed horn at several frequencies in both S and X bands [3]. However, no experimental measurements for the beam pattern of the full antenna have been documented. The aim of this work is to characterize the near-field and far-field beam pattern of the telescope in X-band by using a direct method.

The experiment for the characterization of the beam required the use of a signal generator as the radio frequency (RF) source, due to the fact that celestial sources are not bright enough for the detection of sidelobes. The RF source was initially located and fixed within the near-field distance of the telescope and afterwards relocated beyond the Fresnel zone. By measuring the received power at different positions of the telescope, we were able to characterize the beam pattern.

Section 2 describes the methodology applied in this investigation, followed by the results in Section 3 and conclusions in Section 4.

2. Methodology

There are several methods to measure the beam pattern of an antenna [4]. We use a direct method where we place an RF transmitter at a fixed position away from the telescope, measuring the received power at different positions of the telescope.

For measurement of the beam pattern at the far-field of the telescope, the RF source has to be located beyond the near-field region, whose boundary is given by the Fraunhofer distance as stated in Equation 1:

$$R > \frac{2D^2}{\lambda} \quad (1)$$

where R is the distance from the telescope, D is the maximum dimension of the telescope, and λ is the corresponding wavelength for the frequency of operation.

From Equation 1 and by considering the 6-m aperture of the telescope and a frequency of operation of 8.4 GHz ($\lambda \sim 36$ mm), the RF source must be located at least 2 km beyond the telescope. With the additional constraints of line of sight and high elevation (to reduce ground reflection), it becomes difficult or sometimes impossible to use the direct measurement technique with ground-based RF sources.

2.1. Implementation

The first part of the work was deployed within the observatory by placing the RF source tuned at 8.4 GHz at a distance of 115 m from the telescope and by using a horn type antenna. The received RF signal was down-converted to intermediate frequency at 320 MHz (8080 MHz local oscillator), and later up-converted at 799.9 MHz to the base band converter (BBC). The variations of the received power were measured at the upper side band of one BBC, set up to the central frequency of 799 MHz. Instead of measuring digital counts, we obtained the automatic gain control (AGC) values (given in dB) for the BBC which represent the power fluctuations. Afterwards, a background noise measurement was performed (with the RF source off) and subtracted from the data. We implemented an automatic raster scan schedule which allowed us to get measurements step by step in the azimuth direction and with the elevation position pointing toward the source.



Figure 1. (Left) telescope for VLBI at TIGO and (right) location of the transmitter antenna for the far-field beam pattern characterization.

In the second part of the project, the RF source was located beyond the Rayleigh distance for the X-band (~ 2 km). Fortunately, the geography of the area allowed us to place the RF source in an elevated mountain (20 m above the observatory level) at a distance of 2.84 km. The direct line

of sight crossed a valley, therefore reducing ground reflections. The same previous scanning and acquisition strategy was used. Figure 1 shows the 6-m telescope at TIGO and the location of the transmitter antenna used to characterize the far-field beam pattern of the telescope, while Figure 2 shows a satellite image and a geographic profile of the RF path for far-field measurements.

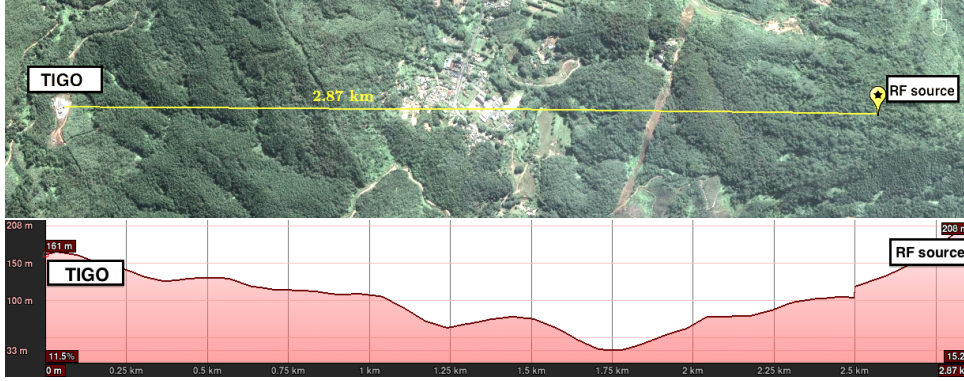


Figure 2. Geographic profile along the RF path for far-field measurements. Credits: GoogleEarth.

3. Results

We present the measured beam pattern after background subtraction and for wide and narrow scanning ranges. The results obtained for the near-field measurements are shown in Figure 3. The wide scanning range was obtained between -100° and $+90^\circ$ with steps of 1° while the narrow scan was obtained for angles $\pm 3.5^\circ$ around the maximum with steps of 0.01° . The elevation angle was approximately 3° for both scans. The main beam data has been fitted with a gaussian function in order to obtain the best estimate of its shape. We observed that the central part of the main beam exhibits a depression, which might be caused by the non-planar wave reaching the reflector due to the short distance between transmitter and receiver. The 3dB beamwidth obtained from the fit was estimated to be 0.8° . However, this behavior is expected given the effects in the near-field and likely affected by ground reflections.

Figure 4 shows the far-field main beam and the wide scanning beam pattern for X-band. The wide scanning was conducted for an azimuth range of $\pm 90^\circ$ around the maximum with steps of 0.5° while the narrow scan was carried out for angles of $\pm 4^\circ$ around the maximum each with samples of 0.01° . Both scans were performed at an elevation angle of approximately 1° . The main beam was fitted with a gaussian function as before. In this case, results show that the estimated 3dB beamwidth $\theta_{3dB} = 0.48^\circ$ is larger than expected from the theory for a large aperture antenna such as the VLBI-TIGO telescope (0.34°). In addition, the first sidelobe has been detected with a level of -10 dB at 0.8° off the center, and a second sidelobe has been detected with a level of -15 dB, at 1.5° off the center. For comparison of the telescope beam pattern, only a computed beam model based on measured feed beam pattern is presented in the documentation of the manufacturer, as shown in Figure 5. The computed model, for feed measurements at 8.57 GHz, shows a first sidelobe of -17.8 dB at 0.8° off the center. The second sidelobes are expected to be below -25 dB and approximately 1.5° off the center.

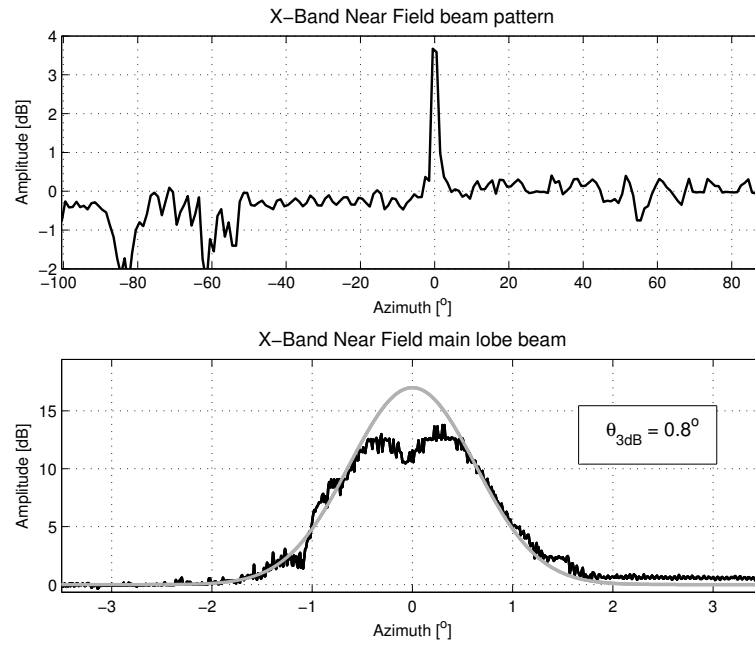


Figure 3. Beam pattern for the wide scanning (top) and narrow beam scanning (bottom) for near-field measurements at 8.4 GHz.

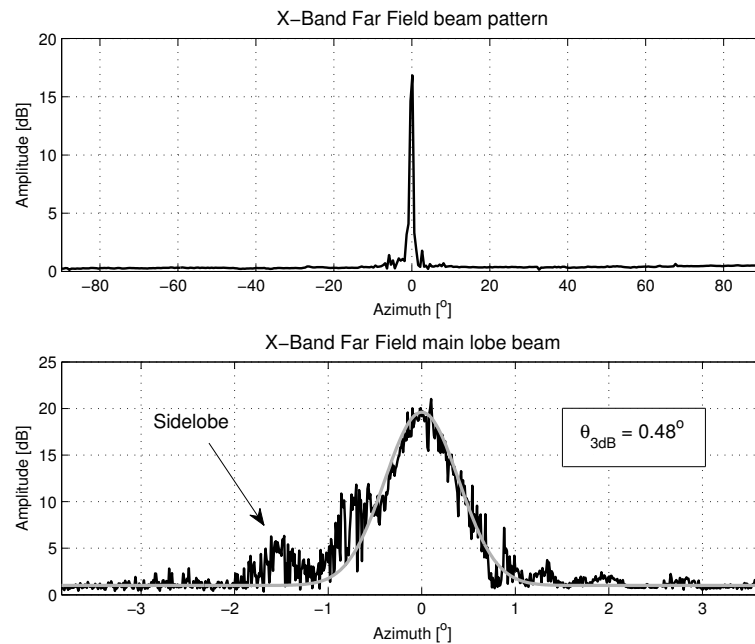


Figure 4. Beam pattern for the wide scanning (top) and narrow beam scanning (bottom) for far-field measurements at 8.4 GHz.

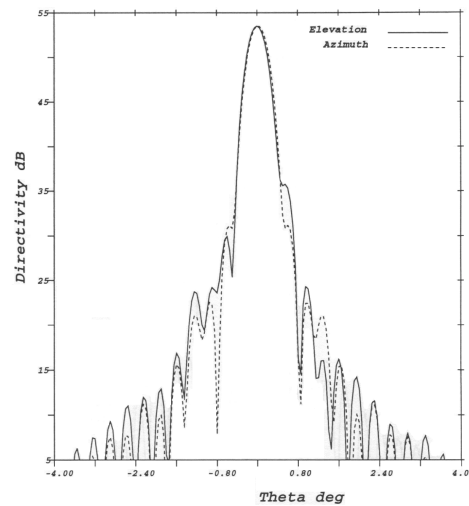


Figure 5. Computed far-field beam pattern at 8.57 GHz (including an ideal 6-m reflector antenna), as provided by the feed manufacturer.

4. Conclusion

An experimental characterization of the near-field and far-field beam pattern of the 6 m TIGO telescope has been developed. Results have shown that the near-field beam pattern does not fit the report by the manufacturer, although this behavior can be expected due to the field effects in this region. The measured far-field beam pattern is close to the expected computed beam (see Figure 5), although the first sidelobe was measured with a level at only 10 dB below the maximum, i.e., approximately 7 dB above the expected level. Moreover, a second sidelobe was measured with a level of 10 dB above the expected value. However, unlike the computed beam pattern, it appeared only at one side of the central peak (non-symmetrical sidelobe) so that it could be caused by surrounding reflections or misalignments. The estimated beamwidth is larger than the theoretical value but close to that obtained from the computed beam pattern.

The impact of the high level sidelobes over the performance of the telescope, and a review of the systematics error of the applied technique, are both subjects of future works.

Acknowledgements

We want to thank the strong collaboration of Exequiel Campillo, Professor Jorge Carranza, the Departamento de Ingeniería Eléctrica undergraduate students, and the entire TIGO staff.

References

- [1] John D. Kraus, *Antennas*, 2nd edition, McGraw-Hill, 1997.
- [2] Hase, H., Transportable Integrated Geodetic Observatory, In: International VLBI Service for Geodesy and Astrometry 1999 Annual Report, NASA/TP-1999-209243, N. R. Vandenberg (ed.), 110-114, 1999.
- [3] TIGO Antenna Feed Chain - Test Report, ERA Document No. ERA/TIG/0505/RPT/3, Issue 1, 9 June 1995.
- [4] IEEE Standard Test Procedures for Antennas, IEEE Std. 149-1979, 2008.